JOURNAL OF CATALYSIS **173,** 450–459 (1998)
ARTICLE NO. CA971920

Catalytic Hydrogen Treatment of Aromatic Alcohols

Eun-Jae Shin and Mark A. Keane[1]

Department of Chemical Engineering, The University of Leeds, Leeds LS2 9JT, United Kingdom

Received July 4, 1997; revised September 15, 1997; accepted September 15, 1997

The gas phase hydrogenation/hydrogenolysis of phenol over the temperature range 423 K $\leq T \leq$ 573 K has been studied using a 1.5% w/w Ni/SiO_2 catalyst. The effects on reaction rate and product selectivity of varying such process variables as reaction time and temperature, contact time, phenol and hydrogen partial pressures, and the phenol solvent were considered. Hydrogenation was observed to occur in a stepwise fashion where the selective formation of the intermediate, cyclohexanone, was promoted at low hydrogen partial pressures and high temperatures, while hydrodeoxygenation to benzene proceeded at temperatures in excess of 523 K. The catalytic hydrogen treatment of cyclohexanone and cyclohexanol, under identical reaction conditions, was examined in order to establish the reaction mechanism. The observed conversions and selectivities are compared to those calculated from equilibrium constant data and it is shown that reaction equilibria are prevalent on the catalyst surface where the equilibrium is shifted to complete hydrogenation to cyclohexanol. The overall reaction is first order in phenol and the apparent dependency on hydrogen concentration increased with increasing temperature. Process selectivity is interpreted in terms of reactant/catalyst interactions where phenol adsorption is viewed as occurring via the aromatic π-electron system and/or the hydroxyl substituent where the latter interaction promotes hydrogenolysis as a direct loss of selectivity with respect to cyclohexanone formation. The hydrogen treatments of the three isomers of cresol were also considered for comparative purposes where the turnover frequency decreased in the order phenol $\geq$ *m*-phenol > *p*-cresol > *o*-cresol; reactivity and selectivity trends are accounted for in terms of electronic and steric effects.

INTRODUCTION

The stringent statutory regulations that now govern the handling of hazardous organic substances present in many industrial waste streams have accelerated the need to establish effective treatment technologies (1). Thermal and/or catalytic oxidations are the widely favoured air pollution abatement techniques, offering high destructive efficiency (2, 3). To ensure a continuous and complete destruction of the hazardous chemicals, a conservative design of the combustion process is necessary which has resulted in complex, oversized, and costly combustion units; products of incomplete combustion (PIC) can include organic acids, aldehydes, CO, amines, etc., depending on the nature of the incinerator feed (4, 5). In order to minimise environmental effects and conserve resources, the first abatement option that should be considered is the recovery and reuse of raw materials. Catalytic hydrogen treatment is proposed here as a viable alternative to thermal/catalytic incinerations for transforming hazardous substances into useful products. Catalytic hydroprocessing has long been used in industry for hydrorefining petroleum but the application of this methodology to the detoxification of organic hazardous wastes has not yet been fully explored (6). In a pilot plant study, Kalnes and James (7) have successfully hydroprocessed some hazardous liquid organic wastes and demonstrated the economic and environmental advantages of hydrotreatment compared with thermal incineration. Aromatic alcohols such as phenol and cresol originate from natural as well as industrial sources and are part of the many hazardous organic compounds present in coal, tar, and petroleum (8). Effluents from coke ovens, oil refineries, petrochemical units, polymeric resin manufacturing, and plastic units contain such aromatic alcohols in large quantities (9). These emissions are of major concern because of their persistence in air and toxicity to all life forms (10) and phenol entry into the environment is now regulated in terms of mpc (maximum permissible concentrations) by the World Health Organisation (WHO) and a number of environmental agencies (11).

The hydrogenation of phenol in the gas (12–18) and liquid (19, 20) phase has been reported, in the main, for a range of palladium (12, 13, 15–17, 20, 21) and platinum (12, 14, 18) based catalyst systems where the emphasis was placed on the selective production of cyclohexanone, a key material in the manufacture of nylon 6 and polyamide resins (21). The use of nickel catalysts has been considered to a far lesser extent (22, 23). A variety of activity/selectivity responses to changes in such process variables as reaction time (13, 15–17), temperature (12, 13, 15, 16, 24), and reactant(s) concentration (12, 13, 16, 17, 22) for the diverse catalyst systems are documented in the literature. The role of

[1] To whom correspondence should be addressed. Fax: +44-113-2332405. E-mail: chemaak@leeds.ac.uk.

0021-9517/98 $25.00

metal loading has also been considered (13, 14, 16–18, 22), and limited kinetic information is available in the form of reaction orders (13, 16) and activation energies (24). It is, however, fair to state that comprehensive kinetic and mechanistic studies are still required to fully assess the feasibility of catalytic hydrogenation/hydrogenolysis as a waste minimisation/pollution abatement methodology. The gas phase hydrogen treatment of phenol over a well-characterised Ni/SiO_2 catalyst (25, 26) is reported in this paper. The effects of reaction time and temperature, reactant(s) partial pressure(s), and contact time on product distribution have been examined, and reproducible turnover frequencies are quoted as part of a kinetic and mechanistic study. The variation of overall reactivity and selectivity due to the presence of a methyl substituent (*o*-, *m*-, and *p*-cresols) has been considered and the role of the reaction solvent is addressed. This paper represents a fundamental study of the catalytic hydrogen treatment of phenols and will form the basis for a future feasibility study of hydrodechlorination as a viable methodology in the treatment of the highly toxic (27) chlorophenols.

EXPERIMENTAL

Catalyst Preparation and Activation

The catalyst was prepared by the homogeneous precipitation/deposition of nickel onto a nonporous microspheroidal Cab–O–Sil 5*M* silica of surface area 194 $m^2\,g^{-1}$ as described in detail elsewhere (25, 28). The nickel loading was determined by atomic absorption (Perkin–Elmer 360 AA spectrophotometer) and the water content by thermogravimetry as outlined previously (29). The hydrated sample, sieved in the 150–200 μm mesh range, was reduced, without a precalcination step, by heating in a 100 $cm^3\,min^{-1}$ stream of dry hydrogen (99.9%) at a fixed rate of 5 K min^{-1} (controlled using a Eurotherm 91e temperature programmer) to a final temperature of 673 ± 1 K which was maintained for 18 h. The catalyst activation procedure and characterisation by carbon monoxide chemisorption and transmission electron microscopy are given a full treatment elsewhere (25, 28).

Catalytic Procedure

All of the catalytic reactions were carried out under atmospheric pressure in a fixed bed glass reactor (i.d. = 15 mm) over the temperature range 423–573 K. The catalyst was supported on a glass frit and a layer of glass beads above the catalyst bed ensured that the reactants reached the reaction temperature before contacting the catalyst. The reactor temperature was monitored by a thermocouple inserted in a thermowell within the catalyst bed; reactor temperature was constant to within ± 1 K. The catalytic reactor has been described previously in some detail (26, 30). A Merck–Hitachi LC-6000A pump was used to deliver the organic feed at a fixed rate which has been carefully calibrated, and the vapour was carried through the catalyst bed in a stream of purified hydrogen. Alcoholic solutions (normally methanolic) of phenol and, for comparative purposes, methanolic solutions of cyclohexanol, cyclohexanone and *o*-, *m*-, and *p*-cresol were used as feedstock where the aromatic concentration was in the overall range 2×10^{-4}–0.3 mol h^{-1}. The catalytic measurements were made at an overall space velocity of 560–2250 h^{-1} (STP) and at W/F values in the range 17–2.2×10^3 g mol^{-1} h where W is the weight of activated catalyst and F is the flow rate of the aromatic. Under these conditions, the catalyst system has been shown to operate with negligible internal or external diffusion retardation of reaction rate (26). The reaction order with respect to hydrogen in the conversion of phenol was determined by dilution in helium to vary the hydrogen partial pressure in the range 0.4–0.8 atm; the reaction order with respect to phenol was likewise evaluated by varying the aromatic partial pressure in the range 0.01–0.15 atm. The reactor effluent was frozen in a liquid nitrogen trap for subsequent analysis, which was made using an AI Cambridge GC94 chromatograph equipped with a flame ionization detector and employing a DB-1 50 m $\times$ 0.20 i.d., 0.33 μm capillary column (J&W Scientific). Data acquisition and analysis were performed using the JCL 6000 (for Windows) chromatography data system and the overall level of reactant hydrogenation/hydrogenolysis was converted to mol% conversion using calibration plots for each feedstock. Mol% conversion is defined as $(m_i - m_o)/(m_i) \times 100$ where m_i is the initial concentration or number of moles of reactant entering the reactor per unit time and m_o is the number of moles of product exiting the reactor per unit time. Molar selectivity in terms of product x is defined by $m_x/m_{tot} \times 100$ where m_{tot} is the total number of moles of product. All the reactants were AnalaR grade and were used without further purification.

RESULTS AND DISCUSSION

Effect of Varying Reaction Conditions

The catalyst precursor has a nickel loading of 1.5% w/w and low water content (<1% w/w). Under the stated activation conditions, the chemisorption data yield a nickel metal dispersion equal to 73% which represents an estimated average nickel particle size of 1.4 nm and a metal surface area of 74 $m^2\,g^{-1}$. Transmission electron microscopy analysis of the activated catalyst (25) supports the chemisorption data and revealed a narrow nickel metal particle size distribution. One batch of this catalyst was used to generate all the catalytic data presented in this paper which represents time-on-stream in excess of 500 h over the temperature interval 423 K $\leq T \leq$ 573 K, processing a range of hydrogen/organic combinations with no appreciable loss of

catalytic activity. The hydrogen treatment of phenol in the presence of the nickel catalyst generated cyclohexanone and cyclohexanol as the products of aromatic ring reduction while benzene was generated at temperatures in excess of 523 K via hydrogenolysis of the hydroxyl substituent. Trace amounts (<1 mol%) of cyclohexane were also isolated in the product mixture. Passage of phenol in a stream of hydrogen through a fixed bed of glass beads (in the absence of Ni/SiO_2) over the same temperature range did not result in any measurable transformation of phenol. Previous reports have revealed a dependence of reaction rate (24) and process selectivity (22) on contact time. In this study, the phenol turnover frequency (number of molecules converted per second per active site) and the product selectivity were found to be constant with variations in contact time (within experimental error) over the range 4×10^{-4}–18×10^{-4} h and all subsequent catalytic data were obtained at the intermediate value of 9×10^{-4} h. Moreover, the short-term deactivation reported for palladium systems (13, 15–17) was not observed in this study where catalytic activity and selectivity were both essentially time invariant and steady state conversion was readily achieved and maintained. In the only directly comparable catalytic study (22), the quoted rate (per gram of catalyst) of phenol conversion over a higher loaded (9% w/w) nickel-on-silica was less than half that recorded in this laboratory. It has, however, been recognised (22) that phenol hydrogenation activity increases with increasing dispersion where the smaller supported nickel particles are the more active. The catalyst used in this study was prepared by homogeneous precipitation/deposition and has been shown to exhibit stronger metal/support interactions than is the case with impregnated catalysts, which results in the formation of smaller nickel metal crystallites with a narrow size distribution (25). The generation of such a well-dispersed nickel metal phase can be considered to be the source of the higher reaction rates generated in this study.

Variations in reaction temperature, however, had a considerable effect on reaction selectivity, as illustrated in Fig. 1. At 423 K, the hydrogen treatment of phenol generated cyclohexanol as by far the predominant product ($S > 98\%$) but with an increase in temperature cyclohexanone formation was increasingly promoted and was the preferred product at the highest temperatures (>540 K) considered. Similar temperature effects have been reported for palladium systems (12, 15) but the data generated in this study are in conflict with a previous report wherein temperature had a negligible effect on selectivity for nickel catalysts (22). Hydrogenolysis of the substituent C–OH bond to form benzene is energetically more demanding and was only initiated and promoted at temperatures greater than 523 K, as has been observed in the hydrogen treatment of other oxygenated aromatics (31, 32). The overall hydrogenation of phenol to cyclohexanol has been viewed as occurring in a stepwise fashion with cyclohexanone as a reactive intermediate (12, 13). The equilibrium constants for the hydrogenation of phenol to cyclohexanone and cyclohexanone to cyclohexanol are available in the literature (15, 33, 34) and are given below in the form of temperature dependencies:

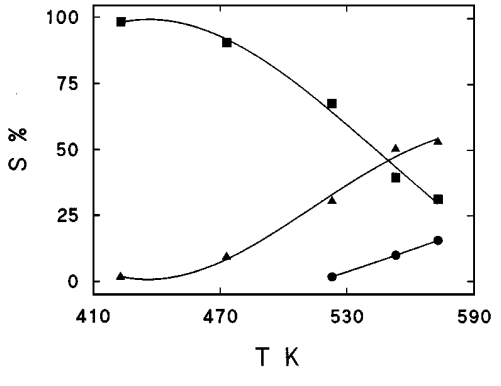

FIG. 1. Selectivity with respect to cyclohexanol (■), cyclohexanone (▲), and benzene (●) formation as a function of temperature.

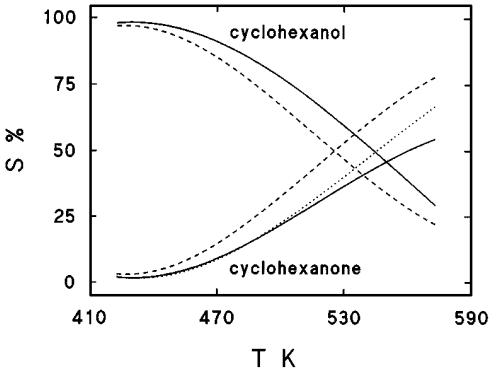

FIG. 2. The temperature dependence of the observed (solid lines) and calculated equilibrium (dashed lines) phenol hydrogenation selectivities with respect to cyclohexanone and cyclohexanol formation: the dotted line represents the combined cyclohexanone + benzene selectivity generated via catalysis.

$$C_6H_5OH + 2H_2 \overset{K_1}{\rightleftharpoons} C_6H_{10}O,$$

$$K_1 = \frac{P_{C_6H_{10}O}}{(P_{C_6H_5OH})(P_{H_2})^2} = 2.7604 \times 10^{-16} \exp\left(\frac{20131}{T}\right), \quad [1]$$

$$C_6H_{10}O + H_2 \overset{K_2}{\rightleftharpoons} C_6H_{11}OH,$$

$$K_2 = \frac{P_{C_6H_{11}OH}}{(P_{C_6H_{10}O})(P_{H_2})} = 3.6844 \times 10^{-7} \exp\left(\frac{7897}{T}\right). \quad [2]$$

Using these equilibrium constants the equilibrium product compositions were calculated at representative temperatures, and the resultant reaction selectivities in the hydrogenation of phenol are compared in Fig. 2 with those generated in this study. The selectivities generated from equilibrium constant calculations and experimental

catalysis exhibit the same pattern in that cyclohexanone formation is promoted with increasing temperature in both cases. At the lower reaction temperatures (<453 K), the equilibrium product distribution generated via heterogeneous catalysis is essentially the same as that which is calculated for the homogeneous gas phase system. At higher reaction temperatures, the two systems diverge and the nickel catalyst clearly shifts the equilibria shown in Eqs. [1] and [2] fully to the right, i.e., complete hydrogenation to cyclohexanol; a constant temperature differential of 20 K is observed for cyclohexanol selectivities in the range 40–75%. The selective formation of cyclohexanone is consistently lower for the catalytic system, with a marked divergence at temperatures greater than 523 K. The latter effect can be accounted for when the additional conversion of phenol to benzene is incorporated into the selectivity plot. The dotted line in Fig. 2 represents the combined selectivity with respect to cyclohexanone and benzene formation and this profile is characterised by a corresponding displacement of 20 K from the calculated line where $T \geq 490$ K. In other words, in what appears to be an equilibrium hydrogenation of phenol on the catalyst surface, the selective formation of the partially hydrogenated cyclohexanone is sacrificed as the hydrogenolysis step is promoted. The equilibrium formation of the fully hydrogenated cyclohexanol is, however, not noticeably disrupted due to this secondary reaction when compared to the theoretical equilibrium. The degree of conversion of the phenol feed is compared to that which is expected under noncatalysed equilibrium conditions in Fig. 3. The conversion in both cases declines at elevated temperatures but the presence of the catalyst ensures

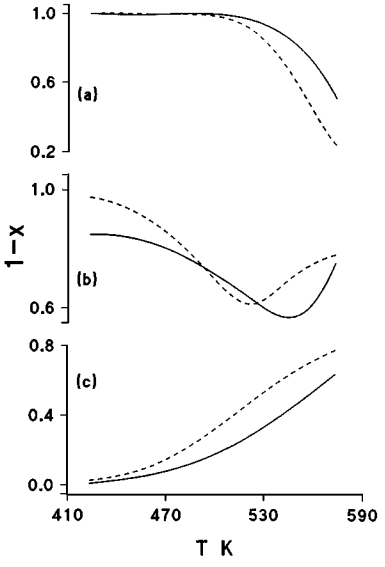

FIG. 3. Effect of reaction temperature on the degree of (a) phenol, (b) cyclohexanone, and (c) cyclohexanol conversion generated in the catalytic step (solid lines) and calculated from equilibrium constants (dashed lines): *x*, mole fraction.

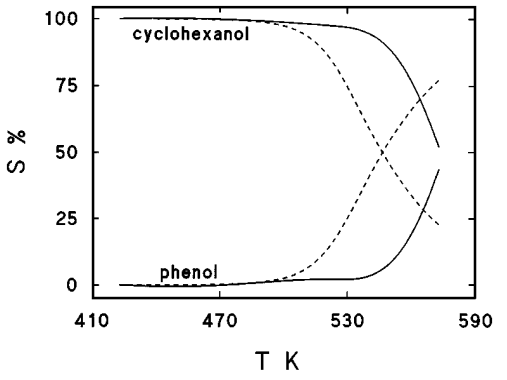

FIG. 4. The temperature dependence of the observed (solid lines) and calculated equilibrium (dashed lines) cyclohexanone hydrogenation/dehydrogenation selectivities with respect to cyclohexanol and phenol formation.

a consistently higher degree of conversion (by up to a factor of 2.1) as a direct result of a greater shift in the equilibrium to full hydrogenation. The drop in activity with increasing temperature has been reported previously (12, 13, 15, 16) and has been attributed to a temperature-induced decrease of the fraction of the catalyst surface that is covered by reactants (13). In this study, however, the observed temperature activity dependency mirrors that predicted from the thermodynamic equilibrium and may be attributed to the thermodynamic constraints where the catalyst serves to extend conversion at elevated (>523 K) temperatures by promoting full hydrogenation to cyclohexanol and hydrogenolysis to benzene.

Kinetic and Mechanistic Studies

Cyclohexanone and cyclohexanol were used as feed under reaction conditions identical to those of the phenol hydrogenation procedure in order to probe the overall reaction network. Reaction selectivity and conversions are compared to the equilibrium calculations in Figs. 3–5. In

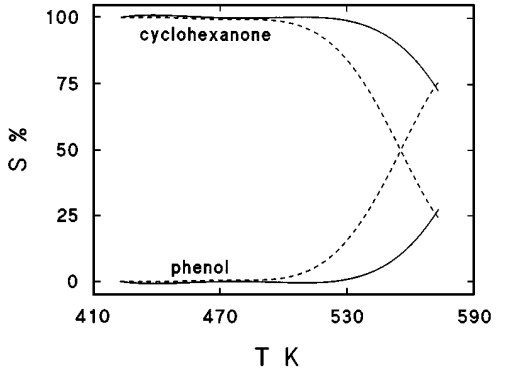

FIG. 5. The temperature dependence of the observed (solid lines) and calculated equilibrium (dashed lines) cyclohexanol dehydrogenation selectivities with respect to cyclohexanone and phenol formation.

the case of the hydrogen treatment of cyclohexanone, the observed selectivities again show a pattern similar to that predicted using the thermodynamic data in that cyclohexanol is the preferred product at lower temperatures with a shift in selectivity in favour of the dehydrogenated product (phenol) at higher temperatures. At temperatures in excess of 500 K, the catalytic system exhibits markedly higher (differentials up to 50%) selectivities with respect to cyclohexanol where the profiles are consistently shifted by 30 K to higher temperatures. It can be stated that the presence of the nickel catalyst significantly shifts the equilibrium to the hydrogenated (cyclohexanol) product. The predicted equilibrium conversion of cyclohexanone falls with increasing temperature to pass through a minimum at 523 K as a direct consequence of the different temperature dependencies of K_1 and K_2 where the dehydrogenation step begins to predominate at higher temperatures and phenol is the favoured product. It is evident from Fig. 3b that the catalytic system shows the same response, which again suggests that the nickel promoted hydrogenation/dehydrogenation process is in equilibrium, but the temperature-related activity minimum appears at a higher temperature (ca. 540 K) due to the overall shift in favour of hydrogenation. Selectivity in terms of the catalytic conversion of cyclohexanol also mimicked that predicted, as shown in Fig. 5. The dehydrogenation reaction occurs stepwise where cyclohexanone formation is first preferred and complete dehydrogenation to phenol is increasingly favoured at the higher temperatures. Whereas there is a clear thermodynamically predicted switch in selectivities at ca. 560 K, the nickel catalyst exhibited a consistently higher selectivity with respect to cyclohexanone formation at every temperature that was studied. The greater shift in the equilibrium to full hydrogenation of phenol, revealed in Fig. 2, is accompanied by an inhibition of the full dehydrogenation of cyclohexanol and the degree of dehydrogenation of the alcohol is lower than the predicted values at every temperature that was considered, Fig. 3c. In addition, the yield of benzene, generated in the catalytic study, from the three reactants increased in the order cyclohexanol < cyclohexanone $\ll$ phenol, which is a direct consequence of the increasing concentration of surface phenol that is available for the hydrogenolysis step.

The kinetics for the hydrogen treatment of phenol may be represented by the power equation

$$\mathrm{TOF} = k P^{m}_{\mathrm{C_6H_5OH}} P^{n}_{\mathrm{H_2}}, \qquad [3]$$

where k represents the rate constant and m and n represent the orders of the reaction with respect to the phenol and hydrogen partial pressures, respectively. The reaction orders were determined by means of logarithmic plots where, for instance, at constant reaction temperature and partial pressure of hydrogen,

$$\log \mathrm{TOF} = \log\left(k P^{n}_{\mathrm{H_2}}\right) + m \log P_{\mathrm{C_6H_5OH}}, \qquad [4]$$

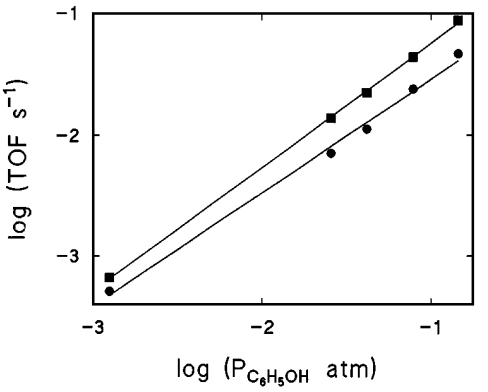

FIG. 6. Turnover frequency of phenol as a function of phenol partial pressure at 423 K (■) and 573 K (●).

and representative logarithmic plots depicting the variation of TOF with the partial pressure of phenol at 423 and 573 K are shown in Fig. 6. The computed reaction order with respect to phenol is one for both temperatures. Values of 1 and −1 (at 433 K) have been quoted previously for Pd/Al_2O_3 (13) and Pd/MgO (16), respectively. By comparison, in the hydrogenation of benzene and methylbenzenes over the same nickel/silica (26, 30) and nickel/zeolite (35, 36) catalysts, the reaction order with respect to the aromatic was observed to increase from 0 to 0.4 in the temperature range 393 K $\leq T \leq$ 523 K. Benzene is known to be adsorbed on nickel catalyst via π-bond interactions in which the aromatic ring lies parallel to the active surface (37, 38). It has been shown that the presence of methyl group(s) on the benzene ring stabilises the adsorbed π-complex with the resultant introduction of a higher energy barrier for aromatic ring hydrogenation (26, 30, 36, 39). The increase in the reaction order with respect to the aromatic at higher temperatures has been attributed to a decrease in the surface coverage by the reactant(s) (26, 30). A temperature invariant reaction order of one with respect to phenol can be considered to be diagnostic of a much weaker interaction than has been observed for benzene or methylbenzene(s). It has been proposed that the stability of the adsorbed π-complex increases (and reactivity consequently decreases) with decreasing ionisation potential (40). The ionisation potential (41) of phenol (8.51 eV) is appreciably lower than that of benzene (9.24 eV) or toluene (8.82 eV) and is within the range of values (8.44–8.58 eV) quoted for the xylenes. In terms of the π-complex stabilities, the expected order of decreasing ease of ring hydrogenation is then benzene > toluene > phenol $\approx$ xylenes. The observed (under identical reaction conditions) TOFs, recorded in Table 1, reveal a markedly higher rate (by a factor of 2.5) of phenol hydrogenation compared with benzene. It is instructive to note that the hydrogen treatment of benzyl alcohol over the same catalyst only generated products of hydrogenolysis (toluene and benzene) while the aromatic ring

TABLE 1

Comparison of the Turnover Frequencies of a Number of Aromatic Reactants under Identical Reaction Conditions: $T = 473$ K

Aromatic reactant	10^3 TOF s^{-1}
Benzene	8.9
Toluene	5.0
o-Xylene	3.5
m-Xylene	4.2
p-Xylene	4.7
Phenol	22.2
o-Cresol	13.9
m-Cresol	21.9
p-Cresol	18.1

remained intact (32). This observation supports the conclusions of Moreau *et al.* (42) that hydrogenolysis activity is higher for slightly electron-donating groups (such as benzyl alcohol, IP = 9.14 (41)) whereas hydrogenation activity is enhanced by strongly electron-donating substituents as is the case with phenol. The higher activity and higher reaction order in the case of phenol suggests a mode of adsorption different from that of the nonoxygenated aromatic reactants. In addition to aromatic ring interactions, phenol can also adsorb on the active surface via the hydroxyl substituent (43, 44) where the aromatic ring is coplanar with (43) or perpendicular to (44) the catalysts surface. The sequence of decreasing hydrogenation rate for the methyl substituted benzene systems, i.e., toluene > *p*-xylene > *m*-xylene > *o*-xylene, has been attributed to an increasing strength of interaction with the surface due to a combination of electronic and steric effects. The methyl-substituted phenols (cresols) exhibit lower turnover frequencies than phenol where the observed order of decreasing reactivity, phenol ≥ *m*-cresol > *p*-cresol > *o*-cresol, is in agreement with that reported previously for the liquid phase batch hydrogenation using palladium catalysts (20). It should be noted that the rate sequence, in the case of the aromatic alcohols, follows the order of increasing pK_a values (41) for phenol and the *m*- and *p*-isomer, i.e., phenol (9.99)∼*m*-cresol (10.00) < *p*-cresol (10.26). The exception to this trend is the *o*-isomer ($pK_a = 10.26$) which exhibits lower TOFs. Such a relationship between rate and the acid ionisation constant suggests that in the case of phenol, *p*-, and *m*-cresol, the ease of hydrogenation can be related to the stability of the associated phenoxide ion in solution. If this represents a valid interdependence, then the gas phase hydrogenation is promoted by phenoxide/catalyst interactions. Ring substituents can have marked effects on the reactivity of phenols by means of inductive and/or resonance effects where a methyl substituent is "electron-releasing" towards the aromatic ring and serves to destabilise phenoxide ion-contributing structures (45). The lower rate of *p*-cresol hydrogenation may then be attributed to a decrease in the contribution of phenoxide/catalyst interactions to the overall reactivity of the system where the effect is inductive. The additional loss of activity in the conversion of the *o*-isomer may be rationalised in terms of steric hindrance and increased ring resonance due to the electron donation to the ring. The latter effect serves to lower the reactivity in a coplanar arrangement of the reactant on the surface where a two-point interaction of the reactant (via aromatic ring and substituent) is envisaged. Alcoholic solutions of phenol were used as feed where there was no detectable product resulting from a reaction between phenol and the solvent. The nature of the alcoholic solvent can, however, have an effect on the ultimate hydrogenation rate as shown in Table 2. While methanol-, ethanol-, and 1-butanol-based feed generated equivalent turnover frequencies, there is a definite solvent dependency for the higher straight chain alcohols. A solvent effect has been reported previously (20) for a liquid phase batch hydrogenation using Pd–C catalysts where the rate was lower in polar solvents, and this effect was attributed to a solvation around the phenoxide ion which weakened adsorption. The opposite trend is evident in this study of a gas phase continuous flow system. If the equilibrium formation of the phenoxide ion in solution is greater in the more polar alcoholic solvents (methanol, ethanol, and 1-butanol) and the dissociation equilibrium is less favoured as the polarity of the alcohol decreases (in the order: 1-pentanol; 1-hexanol; 1-heptanol) and this effect is prevalent and is maintained in the gas phase, then the contribution of phenoxide ion interactions is greater in the former case. It would appear from the activity sequence in Table 2 that the interaction of phenol with the catalyst via the substituent oxygen is the principal source of phenol activation. The same must be true for *p*- and *m*-cresol, and the role of direct aromatic ring activation is more significant for the *o*-isomer due to steric effects.

The variation of process selectivity with phenol partial pressure, illustrated in Fig. 7, sheds some light on the possible mode(s) of phenol adsorption. The equilibrium constant calculations predict a selectivity invariance with phenol concentration, and this is indeed the case at lower reaction temperatures where the only products formed are the result

TABLE 2

Effect of Varying the Nature of the Alcoholic Solvent on the Overall Turnover Frequency of Phenol: $T = 473$ K

Solvent	10^2 TOF s^{-1}
Methanol	2.2
Ethanol	2.1
1-Butanol	2.3
1-Pentanol	1.5
1-Hexanol	1.2
1-Heptanol	1.0

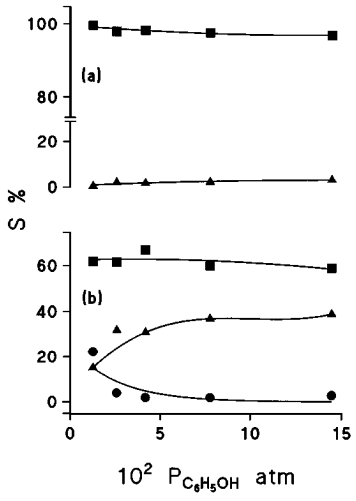

FIG. 7. Selectivity with respect to cyclohexanol (■), cyclohexanone (▲), and benzene (●) formation as a function of phenol partial pressure at (a) 423 K and (b) 573 K.

of hydrogenation. At higher reaction temperatures cyclohexanol formation was again largely independent of phenol partial pressure but the formation of cyclohexanone was certainly enhanced at the direct expense of benzene where the partial pressure of phenol exceeded 0.05 atm. This seeming competition between partial hydrogenation and hydrogenolysis augments the data presented in Fig. 2 and may be accounted for in terms of aromatic/catalyst interactions. Neri *et al*. (13) have proposed that the coplanar orientation of phenol on the catalyst favours complete hydrogenation to cyclohexanol whereas the nonplanar arrangement favours a stepwise hydrogenation. It is not possible from the catalytic data alone to conclusively identify the predominant surface arrangement. The data generated in this study support surface hydrogenation/dehydrogenation equilibria where the catalyst promotes complete hydrogenation. The nonplanar mode of adsorption involving a single point of interaction between the hydroxyl substituent and active surface should certainly promote hydrogenolysis. It is tentatively proposed that cyclohexanol formation is promoted by hydrogen addition to phenol adsorbed in a coplanar orientation with probable surface interactions involving both the hydroxyl substituent and the aromatic ring. Incomplete hydrogenation to cyclohexanone also results from such a surface arrangement or alternatively/additionally via the stepwise addition of hydrogen to phenol adsorbed in a nonplanar orientation where at higher temperatures hydrogenolysis is promoted in direct competition with partial hydrogenation. If this is the case then the selectivity dependence of phenol partial pressure suggests that hydrogenolysis, and by inference a nonplanar adsorption of phenol, is favoured at low concentrations of phenol. Reaction selectivity at two representative temperatures for the hydrogen treatment of the three cresol isomers is presented in Table 3 where the data for phenol processing is also included for comparative purposes. Both *p*- and *m*-cresol show similar selectivity trends to phenol in that selective partial hydrogenation and hydrogenolysis are preferred at higher temperatures; in contrast, 1,2-methylcyclohexanone formation from *o*-cresol is less favoured. Hydrogenolysis or hydrodeoxygenation, in the case of *p*- and *m*-cresol, was initiated at the lower temperature of 473 K and was promoted with a greater degree of selectivity than was observed for the phenol feed. Such an increase in hydrogenolysis selectivity can be attributed to an electronic effect where electron donation from the methyl substituent to the ring serves to weaken the C–O bond. The order of reactivity of cresols with respect to hydrodeoxygenation has been reported in the literature to be *m*- > *p*- > *o*-cresol (46, 47). In this study, *m*- and *p*-cresol exhibited essentially the same selectivity in terms of toluene formation and the electronic effect can be considered to be equivalent, under the stated reaction conditions, for CH_3 positioned *p*- and *m*-cresol to the hydroxyl function. The *o*-cresol reactant exhibited lower hydrogenolysis reactivity than phenol, an observation that is both borne out (48) and in direct conflict (49) with earlier reports. Steric hindrance to adsorption due to the proximity of the methyl group in the *o*-isomer has been invoked in a number of hydrogenolysis systems (46, 47, 50) to explain the lower reactivity of this isomer. As the selectivity pattern observed in this study for the processing of *o*-cresol reactant displayed such a deviation from that recorded (in Table 3) for phenol and the remaining isomers, it is proposed that the nature of the reactant/catalyst interaction is different in the former case. The presence of *o*-CH_3 must impede the nonplanar arrangement or rather cant the aromatic ring towards a planar adsorption mode, the result

TABLE 3

Effect of Reaction Temperature on Process Selectivity in the Hydrogen Treatment of Phenol and the Three Isomeric Forms of Cresol

Reactant	*S*% ketone[a]	*S*% alcohol[b]	*S*% aromatic[c]
	$T = 473$ K		
Phenol	9	91	0
o-Cresol	35	65	0
m-Cresol	20	80	<1
p-Cresol	12	88	<1
	$T = 573$ K		
Phenol	53	31	16
o-Cresol	12	80	8
m-Cresol	46	33	22
p-Cresol	40	38	22

[a] Cyclohexanone from phenol and 1,2-, 1,3-, or 1,4-methylcyclohexanone from *o*-, *m*-, and *p*-cresol, respectively.

[b] Cyclohexanol from phenol and 1,2-, 1,3-, or 1,4-methylcyclohexanol from *o*-, *m*-, and *p*-cresol, respectively.

[c] Benzene from phenol and toluene from *o*-, *m*-, and *p*-cresol.

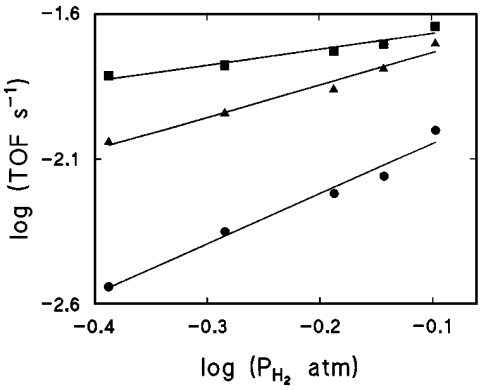

FIG. 8. Turnover frequency of phenol as a function of hydrogen partial pressure at 423 K (■), 523 K (▲), and 573 K (●).

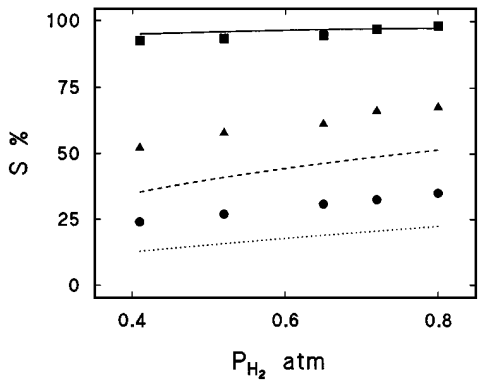

FIG. 9. Effect of hydrogen partial pressure on the observed (symbols) and calculated equilibrium (lines) selective formation of cyclohexanol from phenol at 423 K (■, solid line), 523 K (▲, dashed line), and 573 K (●, dotted line).

being that *o*-cresol exhibits a greater deal of interaction between the catalyst and the aromatic nucleus. Such a surface arrangement will limit the extent of hydrogenolysis and the increase in ring resonance due to electron donation from the methyl substituent means higher energy requirements for complete hydrogenation, which results in the observed shift in selective alcohol formation to higher temperatures.

The reaction order with respect to hydrogen was determined by varying the partial pressure of hydrogen at a constant partial pressure of phenol, employing helium as a diluent and representative logarithmic plots are shown in Fig. 8. The computed reaction order increased with a rise in reaction temperature from 423 K (0.5) to 523 K (1.1) and 573 K (1.7). A reaction order of 2 and 1.3 at 433 K has been reported for Pd/Al_2O_3 (13) and Pd/MgO (13, 16), respectively, where the latter catalyst system exhibited an increase in hydrogen dependency to 1.8 at 473 K (16). Such a temperature-induced increase in hydrogen reaction order has been observed for a range of nickel-promoted aromatic hydrogenation reactions (26, 30, 35, 36, 51). It has been demonstrated elsewhere (26) that such variations in the experimentally determined reaction order are due to the temperature dependence of the surface concentration of hydrogen. A recent chemisorption and TPD study of hydrogen on Ni/Al_2O_3 (52) revealed different hydrogen adsorption states which are strongly dependent on temperature. The greater dependence of the phenol hydrogenation rate on hydrogen partial pressure may then be attributed to an increased mobility and temperature induced loss of surface reactive hydrogen. The effect of hydrogen partial pressure on the selective formation of cyclohexanol and cyclohexanone is illustrated in Figs. 9 and 10, respectively. The observed selectivity with which cyclohexanol was produced decreased with decreasing hydrogen partial pressure and this effect was more pronounced at higher reaction temperatures (Fig. 9). The loss of cyclohexanol selectivity coincides with an increasingly favoured production of cyclohexanone at lower hydrogen partial pressures (Fig. 10); benzene formation was essentially independent of hydrogen concentration. These observations are in qualitative agreement with the earlier finding that cyclohexanone is promoted at lower hydrogen/phenol molar ratios (22). However, at temperatures greater than 423 K, the observed selectivities with respect to cyclohexanone and cyclohexanol formation are consistently lower and higher, respectively, than those predicted thermodynamically. These relationships again illustrate the role of the catalyst in shifting the overall equilibrium towards complete hydrogenation.

A reaction mechanism that accounts for the observed rate data is summarised as

$$C_6H_5OH + A \overset{K_A}{\rightleftharpoons} C_6H_5OH{-}A \qquad [5]$$

$$2H_2 + 4S \overset{K_{4H}}{\rightleftharpoons} 4H{-}S \qquad [6]$$

$$C_6H_5OH{-}A + 4H{-}S \overset{K_1'}{\rightleftharpoons} C_6H_{10}O{-}A + 4S \qquad [7]$$

$$C_6H_{10}O{-}A \overset{K_{1D}}{\rightleftharpoons} C_6H_{10}O(g) + A \qquad [8]$$

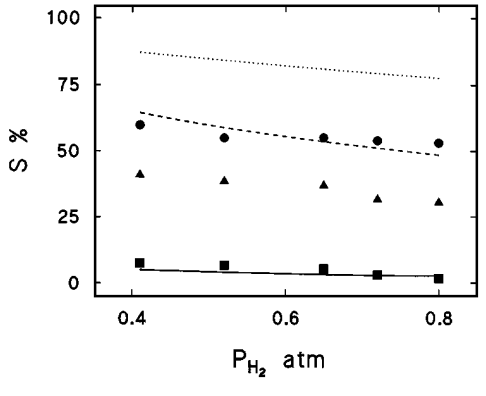

FIG. 10. Effect of hydrogen partial pressure on the observed (symbols) and calculated equilibrium (lines) selective formation of cyclohexanone from phenol at 423 K (■, solid line), 523 K (▲, dashed line), and 573 K (●, dotted line).

$$H_2(g) + 2S \overset{K_{2H}}{\rightleftharpoons} 2H\text{–}S \quad [9]$$

$$C_6H_{10}O\text{–}A + 2H\text{–}S \overset{K_2'}{\rightleftharpoons} C_6H_{11}OH\text{–}A + 2S \quad [10]$$

$$C_6H_{11}OH\text{–}A \overset{K_{2D}}{\rightleftharpoons} C_6H_{11}OH(g) + A, \quad [11]$$

where A and S denote adsorption sites for the aromatic and hydrogen (adsorbed dissociatively) reactants, respectively. The model, in keeping with the earlier study (26) of benzene and methylbenzene(s) hydrogenation, assumes that both reactants adsorb at different sites and the surface reactants and products exist in quasi-equilibrium with the gas phase. The surface hydrogenation reaction proceeds stepwise where partially hydrogenated cyclic alcohols are not isolated in the product stream, tautomerisation of cyclohexene-1-ol to cyclohexanone must occur readily, and the formation of cyclohexanone and cyclohexanol is in equilibrium. The generation of benzene is taken to be an irreversible hydrogenolysis step which lowers the overall selective formation of cyclohexanone:

$$C_6H_5OH\text{–}A + 2H\text{–}S \overset{k_1}{\rightarrow} C_6H_6\text{–}A + H_2O(g) + 2S \quad [12]$$

$$C_6H_6\text{–}A \overset{K_{3D}}{\rightleftharpoons} C_6H_6(g) + A \quad [13]$$

Quasi-equilibria for the adsorption and desorption steps yield, for instance,

$$K_A = \frac{\theta_{C_6H_5OH}}{P_{C_6H_5OH}\theta_A}, \quad [14]$$

$$K_{4H} = \frac{\theta_H^4}{P_{H_2}^2\theta_S^4}, \quad [15]$$

and

$$K_{1D} = \frac{P_{C_6H_{10}O}\theta_A}{\theta_{C_6H_{10}O}}, \quad [16]$$

where θ denotes surface coverage. The equilibrium constant for the surface partial hydrogenation of phenol to cyclohexanone is given by

$$K_1' = \frac{\theta_{C_6H_{10}O}\theta_S^4}{\theta_{C_6H_5OH}\theta_H^4} \quad [17]$$

and the temperature dependence (where $423\,K \le T \le 573\,K$) of this surface-controlled equilibrium is related to the gas phase reactant partial pressures by

$$K_1^* = \frac{P_{C_6H_{10}O}}{P_{C_6H_5OH}P_{H_2}^2} = 4.9 \times 10^{-14} \exp\left(\frac{17960}{T}\right), \quad [18]$$

where

$$K_1^* = K_1'K_AK_{4H}K_{1D}. \quad [19]$$

In the hydrogenation of cyclohexanone to cyclohexanol, the temperature dependence of the equilibrium constants generated by catalysis can likewise be represented by

$$K_2^* = \frac{P_{C_6H_{11}OH}}{P_{C_6H_{10}O}P_{H_2}} = 1.0 \times 10^{-5} \exp\left(\frac{6644}{T}\right), \quad [20]$$

where

$$K_2^* = \frac{K_2'K_{2H}K_{2D}}{K_{1D}}. \quad [21]$$

The deviation in equilibria induced by the nickel catalyst in a continuous flow system can be seen from a direct comparison of Eq. [18] with Eq. [1] and Eq. [20] with Eq. [2].

CONCLUSIONS

The data presented in this paper support the following conclusions:

(i) The hydrogenation of phenol to cyclohexanol proceeds stepwise via the formation of cyclohexanone as a reactive intermediate. The observed rate data are explained by a mechanism involving equilibrated adsorption and hydrogenation steps where the catalyst serves to shift the equilibrium in favour of complete hydrogenation.

(ii) Phenol can adsorb on the catalyst at the aromatic ring and/or the hydroxyl substituent where the latter interaction promotes hydrogenolysis to benzene at the direct expense of cyclohexanone formation.

(iii) Steady state conversion, which is independent of contact time, is readily achieved with no appreciable deactivation after extended (>500 h) use.

(iv) The hydrogenation rate exhibits a temperature invariant first order dependence on phenol concentration and a lower turnover frequency in less polar alcoholic solvents, which is taken to be diagnostic of a predominantly weak interaction with the catalyst that involves phenoxide ion formation.

(v) The reaction order with respect to hydrogen increases with increasing temperature due to an induced loss of catalytically active hydrogen from the catalyst surface where lower hydrogen partial pressure promotes the selective formation of cyclohexanone.

(vi) The sequence of decreasing hydrogenation rate, phenol $\approx$ *m*-cresol > *p*-cresol > *o*-cresol, is attributed to inductive and steric effects where the selectivity pattern generated by the *o*-isomer deviates significantly from the other aromatic alcohols and suggests a different mode of adsorption/activation.

ACKNOWLEDGMENT

E.J.S. acknowledges partial financial support from the British Council.

REFERENCES

1. Joglekar, H. S., Samant, S. D., and Joshi, J. B., *Water Res.* **25**, 135 (1991).
2. van der Vaart, D. R., Marchand, E. G., and Bagely-Pride, A., *Critic. Rev. Environ. Sci. Tech.* **24**, 203 (1994).
3. Noordally, E., Richmond, J. R., and Tahir, S. F., *Catal. Today* **17**, 359 (1993).
4. Cooper, C. D., Clausen, C. A., Tomlin, D., Hewett, M., and Martinez, A., *J. Hazard. Mater.* **27**, 273 (1991).
5. Dial, C. J., *Chem. Eng. Prog.* **82**, 16 (1986).
6. Gioia, F., *J. Hazard. Mater.* **26**, 243 (1991).
7. Kalnes, R. C., and James, R. B., *Environ. Prog.* **7**, 185 (1988).
8. Bhargara, D. S., Bhatt, D. J., and Panesar, P. S., *J. Environ. Eng.* **109**, 369 (1983).
9. Ong, S. K., and Bowers, A. R., *J. Environ. Eng.* **116**, 1013 (1990).
10. Shieh, W. K., Puhakka, J. A., Melin, E., and Tuhkanen, T., *J. Environ. Eng.* **116**, 683 (1990).
11. Bezuglaya, E. Y., Shchutskaya, A. B., and Smirnova, I. V., *Atmos. Environ.* **27**, 773 (1993).
12. Talukdar, A. K., Bhattacharyya, K. G., and Sivasanker, S., *Appl. Catal. A: General* **96**, 229 (1993).
13. Neri, G., Visco, A. M., Donato, A., Milone, C., Malentacchi, M., and Gubitosa, G., *Appl. Catal. A: General* **110**, 49 (1994).
14. Srinivas, S. T., Lakshmi, L. J., and Rao, P. K., *Appl. Catal. A: General* **110**, 167 (1994).
15. Itoh, N., and Xu, W.-C., *Appl. Catal. A: General* **107**, 83 (1993).
16. Galvagno, S., Donato, A., Neri, G., and Pietropaolo, R., *J. Chem. Technol. Biotechnol.* **51**, 145 (1991).
17. Narayanan, S., and Krishna, K., *Appl. Catal. A: General* **147**, L253 (1996).
18. Srinivas, S. T., and Rao, P. K., *J. Chem. Soc. Chem. Commun.*, 33 (1993).
19. Tang, U. M., Hung, M. Y., and Jiang, Y. Y., *Macromol. Rapid Commun.* **15**, 527 (1994).
20. Higashijima, M., and Nishimura, S., *Bull. Chem. Soc. Jpn.* **65**, 2955 (1992).
21. Dodgson, I., Griffen, K., Barberis, G., Pignatora, F., and Tauszik, G., *Chem. Ind.*, 830 (1989).
22. Narayanan, S., and Sreekanth, G., *Ind. J. Technol.* **31**, 507 (1993).
23. Narayanan, S., and Sreekanth, G., *React. Catal. Lett.* **51**, 449 (1993).
24. Gonzalez-Velasco, J. R., Gutierrez-Ortiz, J. I., Gonzalez-Marcos, J. A., and Romero, A., *Kinet. Catal. Lett.* **32**, 505 (1986).
25. Keane, M. A., *Can. J. Chem.* **72**, 372 (1994).
26. Keane, M. A., and Patterson, P. M., *J. Chem. Soc., Faraday Trans.* **92**, 1413 (1996).
27. Hoke, J. B., Gramiccioni, G. A., and Balko, E. N., *Appl. Catal. B: Environmental* **1**, 285 (1992).
28. Keane, M. A., and Webb, G., *J. Catal.* **136**, 1 (1992).
29. Coughlan, B., and Keane, M. A., *J. Catal.* **123**, 364 (1990).
30. Keane, M. A., *J. Catal.* **166**, 347 (1997).
31. Keane, M. A., *Bull. Soc. Chim. Belg.* **104**, 63 (1995).
32. Keane, M. A., *J. Mol. Catal.* **118**, 261 (1997).
33. Chitwood, H. C., Fitzpatrick, J. T., Fowlerand, G. W., and Freure, B. T., *Ind. Eng. Chem.* **44**, 1696 (1952).
34. Cubberley, A. H., and Mueller, M. B., *J. Am. Chem. Soc.* **69**, 1535 (1947).
35. Coughlan, B., and Keane, M. A., *Zeolites* **11**, 12 (1991).
36. Coughlan, B., and Keane, M. A., *Catal. Lett.* **5**, 101 (1990).
37. Minot, C., and Gallezot, P., *J. Catal.* **123**, 34 (1990).
38. Coughlan, B., and Keane, M. A., *J. Chem. Soc., Faraday Trans.* **86**, 3961 (1990).
39. Stanislaus, A., and Cooper, B., *Catal. Rev. Sci. Eng.* **36**, 75 (1994).
40. Völter, J., Hermann, M., and Heise, K., *J. Catal.* **12**, 307 (1968).
41. Dean, J. A., "Handbook of Organic Chemistry." McGraw–Hill, New York, 1987.
42. Moreau, C., Joffre, J., Saenz, C., and Geneste, P., *J. Catal.* **122**, 448 (1990).
43. Taylor, R., and Lundlum, K. H., *J. Phys. Chem.* **76**, 2882 (1972).
44. Tanabe, K., and Nishizaki, T., *in* "Proceedings, 6th International Congress on Catalysis" (G. C. Bond, P. B. Wells, and F. C. Tompkins, Eds.), p. 863. Catalysis Society, Letchworth, 1977.
45. Brown, W. H., "Organic Chemistry." Saunders, New York, 1995.
46. Odebunmi, E. O., and Ollis, D. F., *J. Catal.* **80**, 56 (1983).
47. Rollmann, L. D., *J. Catal.* **46**, 243 (1977).
48. Weigold, H., *Fuel* **61**, 1021 (1982).
49. Bredenberg, J. B., Huuska, M., Räty, J., and Korpio, M., *J. Catal.* **77**, 242 (1982).
50. Gevert, S. B., Eriksson, M., Eriksson, P., and Massoth, F. E., *Appl. Catal. A: General* **117**, 151 (1994).
51. Smeds, S., Murzin, D., and Salmi, T., *Appl. Catal. A: General* **125**, 271 (1995).
52. Smeds, S., Salmi, T., Lindfors, L. P., and Krause, O., *Appl. Catal. A: General* **144**, 177 (1996).